Simultaneous dual-wavelength photoacoustic radar imaging using waveform engineering with mismatched frequency modulated excitation

Bahman Lashkari,[1,*] Sung Soo Sean Choi,[1,2] Mohammad E. Khosroshahi,[1] Edem Dovlo,[1] and Andreas Mandelis[1,2]

[1]*Center for Advanced Diffusion-Wave Technologies (CADIFT), Department of Mechanical and Industrial Engineering, University of Toronto, Toronto M5S 3G8, Canada*

[2]*Institute of Biomaterials and Biomedical Engineering (IBBME), University of Toronto, Toronto, Canada*

**Corresponding author: bahman@mie.utoronto.ca*

Received December 29, 2014; revised February 13, 2015; accepted February 17, 2015; posted February 18, 2015 (Doc. ID 231546); published March 16, 2015

The spectroscopic imaging capability of photoacoustics (PA) without the depth limitations of optical methods offers a major advantage in preclinical and clinical applications. Consecutive PA measurements with properly chosen wavelengths allow composition related information about blood or tissue. In this work, we propose and experimentally introduce modulation waveform engineering through the use of mismatched (uncorrelated or weakly correlated) linear frequency modulated signals for PA characterization and imaging. The feasibility of the method was tested on oxygen saturated hemoglobin and deoxygenated hemoglobin *in vitro* in a blood circulating rig. The method was also employed for *in vivo* imaging of a neck carcinoma tumor grown in a mouse thigh. The proposed method can increase the accuracy and speed of functional imaging by simultaneous PA probing with two wavelengths using portable laser-diode based PA imaging systems.

OCIS codes: (110.0110) Imaging systems; (110.5125) Photoacoustics; (110.5120) Photoacoustic imaging; (170.6510) Spectroscopy, tissue diagnostics; (060.2630) Frequency modulation.

http://dx.doi.org/10.1364/OL.40.001145

Frequency-domain photoacoustic (FD-PA) imaging is an alternative method to conventional pulsed laser PA [1]. The availability of compact and inexpensive high power diode lasers is a major motivator for employing FD-PA in biomedical PA [1]. FD-PA can be performed using either single frequency (depth integrated) [2] or a coded excitation waveform (depth resolved) and has some unique features, such as providing phase information which can be used for image SNR enhancement [3] or tomographic reconstruction [4].

The dependence of the absorption coefficient of materials on irradiation wavelength provides an effective tool for PA functional imaging. This feature has been studied widely for detection of angiogenesis and hypermetabolism, as well as tissue characterization applications such as lipid-rich plaques in the vascular system [5–8]. Typically, the difference in the absorption coefficient of dominant components, such as oxyhemoglobin (HbO_2) and deoxyhemoglobin (HbR) at two wavelengths, is used to reveal each component's concentration which leads to clinically meaningful information regarding hemoglobin oxygen saturation and total hemoglobin concentration. It should be mentioned that it is possible to perform functional imaging using FD-PA and the process is very similar to the conventional pulsed method [9].

In many cases, *in vivo* functional imaging involves moving fluids, such as blood or moving body parts, because of heart beating or breathing. These types of movements introduce errors to sequential PA measurements supposed to be performed *at the same tissue or blood vessel location*. Furthermore, sequential multi-spectral imaging of tissues has been introduced as a means to enhance contrast and improve the diagnosis of tumors [10,11]. For similar reasons, *simultaneous* multi-spectral imaging is a desirable goal toward improved stability and target image reliability. For blood-related diagnosis, to ensure the accuracy of concentration estimation, it is important to perform the PA measurements with two laser wavelengths in a very short time and, ideally, simultaneously. Related work reported by Mienkina *et al.* explored the feasibility of using orthogonal Golay codes for simultaneous multi-spectral PA imaging [12]. Quasi-simultaneous (rapid sequential) functional pulsed laser PA imaging was also performed with two lasers (as well as an ultrasonic pulse) emitting with an inter-laser delay time as short as ~30 μs [13] and, recently in another work, a delay as short as 17 μs, between the two laser pulses [14].

In this Letter, we show that, by using coded excitation, it is possible to perform simultaneous PA probing with two wavelengths. Using mismatched codes enables the receiver to differentiate between various PA signal sources. Ideal mismatched codes are those that generate a very strong autocorrelation and very weak cross-correlation between themselves. In this work, long linear frequency modulation (LFM) chirps were employed to maximize the signal-to-noise ratio (SNR).

The simplest method to generate two mismatched coded excitations is to use two LFM chirps, one of which is up-sweeping and the other is down-sweeping the frequency range [15]. Since the slopes of these frequency sweeps are equal with opposite signs, they create the highest mismatched factor [15]. It should be added that the use of mismatched coded excitations is not limited to two codes. It has been shown that it is possible to generate multiple mismatched coded excitation signals with identical bandwidth and code length [16]. Thus, while sharing the same signal (image) resolution, each wavelength generates its own PA response.

To demonstrate the feasibility of simultaneous dual-wavelength PA probing, the proposed method was applied to oxygen-saturated and deoxygenated sheep blood. Two

CW lasers were employed: an 805 nm diode laser (Laser Light Solutions, New Jersey, USA) and a 680 nm diode (LDX Optronics Inc., Maryville, Tennessee, USA). The 680 nm diode laser was modulated by a high-frequency driver VFM5-25 (MESSTEC, Germany), and the 805 nm diode laser was equipped with its own driver. A dual-channel arbitrary waveform generator (33500B, Agilent Technologies, Inc., Loveland, Colorado, USA) was used to control the drivers. The experiment was performed on a blood circulating rig. A peristaltic pump (Heidolph Instruments GmbH & Co., Germany) was used to circulate heparinized sheep blood (Caderlane Labs, Burlington, Ontario, Canada) continuously from a sealed blood bag to a convertible flow cell (CFCAS0004, IBI Scientific, Peosta, Iowa, USA) and back to the blood bag through plastic tubing (Fig. 1). The output fibers of the two diode lasers were connected to two identical 0.8 mm collimators (F230SMA-B, Thorlabs, New Jersey, USA) which were directed toward the same point on the surface of the measurement unit. The area of the 805 nm laser beam was adjusted with a lens to cover approximately the same area on the surface as the 680 nm laser beam (~15 mm diameter). A focused ultrasonic transducer with 1 MHz center frequency V314 (Olympus NDT Inc., Panametrics, USA) was placed in front of the measurement cell at its focal distance, 1.9 in. The output signal of the transducer was amplified 40 dB (preamplifier 5676, Panametrics, Olympus, USA) before being digitized by a data acquisition card. Signal acquisition and synchronization were performed through a National Instruments system.

First, the blood was exposed to ambient air to become fully oxygen saturated. The laser powers were set to 900 mW (680 nm) and 600 mW (805 nm). The driver of the 680 nm laser was set to an up-sweeping chirp from 300 kHz to 1.3 MHz, and the 805 nm laser was set to down-sweeping the same frequency range. The chirp duration was set to 1 ms and the received signals were averaged over 50 measurements. Thus, the total exposure time for each measurement was 50 ms. The rationale for choosing the specific chirp bandwidth is discussed elsewhere [17]. Both channels of the waveform generator were synchronized with an external trigger generated by the National Instruments system. The PA measurement was subsequently performed three times, once with each laser and the third time with both lasers operating simultaneously. Figures 2(a)–2(c) show the envelope cross-correlation signals of three measurements: (a) 680 nm irradiation only, (b) 805 nm irradiation only, and (c) both lasers emitting together. A comparison between the peak values in the dual-waveform case with each individual

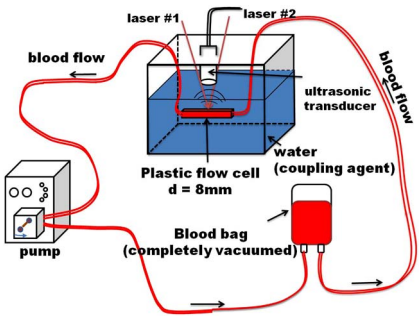

Fig. 1. Blood circulation rig and PA measurement setup.

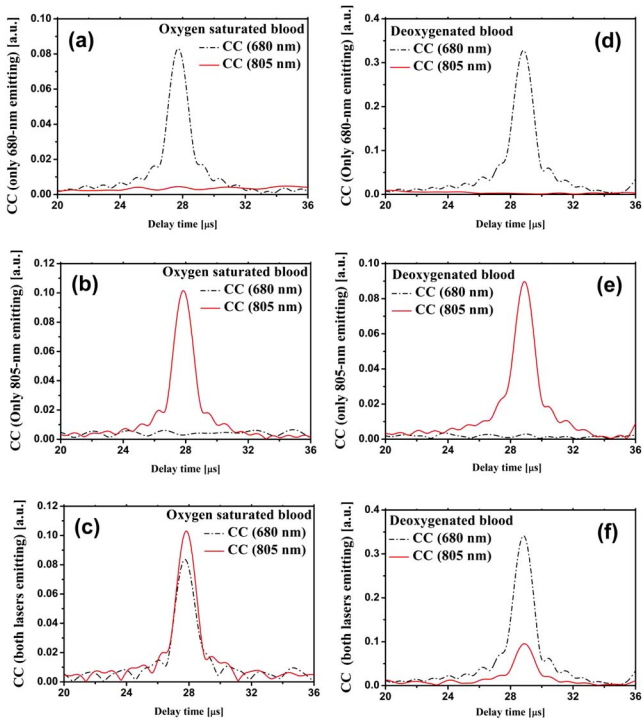

Fig. 2. FD-PA cross-correlation (CC) signals from oxygen saturated blood with irradiation of (a) 680 nm, (b) 805 nm, and (c) both wavelengths. Also shown are cross-correlation signals from deoxygenated blood with irradiation at (d) 680 nm, (e) 805 nm, and (f) both wavelengths. When one laser is off, its corresponding CC in the figure shows the cross-correlation of the associated (up- or down-swept) chirp with the detected signal. These CCs experimentally demonstrate the correlation of the two mismatched chirps.

waveform (when the other laser was off) shows that each signal operates independently of the other signal with minor interaction between them. The variation of peak values in the dual-waveform case compared with the single waveform measurements is –36.8 dB and –43.8 dB for 805 nm and 680 nm wavelengths, respectively. This variation is smaller than the noise level in each single wavelength measurement. On the other hand, the cross-correlation of each signal with the other LFM chirp generates a baseline less than –22 dB [Figs. 2(a), 2(b)]. It should be noticed that this baseline resulting from the cross-correlation between the two waveforms depends on bandwidth and chirp duration. With these parameters increasing, it is possible to decrease the baseline level. Using the molar extinction coefficients of hemoglobin in the employed wavelengths [18], the measured data can readily reveal the hemoglobin oxygen saturation.

By adding sodium dithionite to the oxygenated hemoglobin, we can increase the level of deoxygenation in the blood [19]. We added about 0.4 g of sodium dithionite powder (Sigma-Aldrich, St. Louis, Missouri, USA) to 150 ml of the blood in the container which is enough to completely deoxygenate the blood [19]. After 20 min of blood circulation through the tube loop, we repeated the experiments. The laser power, chirp duration, and number of data acquired for averaging were the same as above. The envelope cross-correlation signals are shown in Figs. 2(d)–2(f) for 680, 805 nm, and simultaneous operation of both lasers, respectively. The variation of

peak values in the simultaneous and single wavelength measurements is −24.6 dB and −28.2 dB for 805 nm and 680 nm operation, respectively. The baselines resulting from cross-correlation with the other chirp are seen in Figs. 2(d) and 2(e) and are −28.7 dB and −27.4 dB, respectively. These small variations confirm that the simultaneously transmitted mismatched codes generated independent responses that were accurately measured.

The percentage of HbO_2 (oxyhemoglobin) and HbR (deoxyhemoglobin) can be obtained from the results presented in Fig. 2. The absorption coefficient in each case can be assumed to be [5]

$$\mu_a(\lambda_i) = \varepsilon_{\mathrm{HbR}}(\lambda_i)[\mathrm{HbR}] + \varepsilon_{\mathrm{HbO_2}}(\lambda_i)[\mathrm{HbO_2}], \quad (1)$$

where ε is the molar extinction coefficient of the corresponding component, and [...] denotes the molar concentration of the component. A key physiological parameter is the blood oxygen saturation (sO_2) which is the percentage of $[HbO_2]$ in the total hemoglobin concentration ($[HbR] + [HbO_2]$)[5]. It is well known that the PA pressure signal is proportional to the Grüneisen parameter (Γ), the laser light fluence (Φ), and the absorption coefficient [5,9]. Therefore, the FD-PA signal should be normalized with the laser intensity in each case. In Eq. (1), the absorption coefficient in each case is proportional to the PA peak divided by the laser intensity. Table 1 shows concentration estimations obtained by substituting the sheep hemoglobin extinction coefficients [18].

In the oxygen saturated case, a blood gas analyzer (CCA_TS, OPTI Medical System, Inc, Roswell, Georgia, USA) was used to measure hemoglobin concentrations independently, and gave the sheep oxyhemoglobin value $sO_2 = 99.5\%$, which means a 6.5% error in the estimates shown in Table 1. In another case, the oxyhemoglobin percentage was less than 60%, a value outside the gas analyzer range. Errors in the foregoing FD-PA blood characterization could have been caused by the following: (1) approximate laser power measurements; (2) noise in the FD-PA measurements even with one wavelength, which may have caused some errors in the estimation of the FD-PA peaks; and (3) the reported values for hemoglobin extinction coefficients may be inaccurate by factors dependent on animal breed, age, gender, and biology.

In another experiment aiming at extending the proof of the validity of the line scan results of Fig. 2 to full multi-wavelength PA images, dual-wavelength PA probing was applied for *in vivo* imaging of a cancerous tumor in a mouse thigh. A nude mouse was purchased from Charles River Laboratories Inc. (Massachusetts, USA). Cultured FaDu cells (human hypopharyngeal head-and-neck squamous cell carcinoma) were injected 21 days prior to the experiment in the right thigh of the mouse.

Table 1. Estimated Oxy- and Deoxy-Hemoglobin Levels

	Sheep Hemoglobin [18]	
Hemoglobin Situation	sO_2 (HbO_2%)	HbR %
Oxygen saturated, Fig. 2(c)	93%	7%
Deoxygenated, Fig. 2(f)	22%	78%

This experiment was performed under the guidelines of animal protocol 20010465 approved by the Division of Comparative Medicine (DCM) of the Faculty of Medicine at the University of Toronto. Animal handling was performed according to the guidelines for care and use in the laboratory. The animal was anesthetized using isoflurane gas, and full anesthesia was maintained throughout the experiment by administrating 1.4 L/min oxygen and 1 L/min isoflurane.

The PA imaging of the mouse thigh was first performed by an in-house imaging system described elsewhere [20]. A 64-element phased array ultrasonic transducer SA4 2/24 (Ultrasonix, British Columbia, Canada) was used. The same laser diodes emitting at 680 and 805 nm were employed with respective powers of 1.3 and 3 W and up- and down-swept chirps in the 300 kHz–4 MHz frequency range. The chirp duration of 1 ms was employed, and each full-chirp signal was averaged 40 times. The mouse leg and the transducer surface were fully submerged in water for acoustic coupling [Fig. 3(a)]. PA imaging was first performed using the 805 nm laser alone and then using both wavelengths emitted simultaneously. After PA imaging as the transducer was fixed in the water tank, its interface was detached from the PA imager and was connected to a commercial ultrasound system (Ultrasonix, British Columbia, Canada) to perform

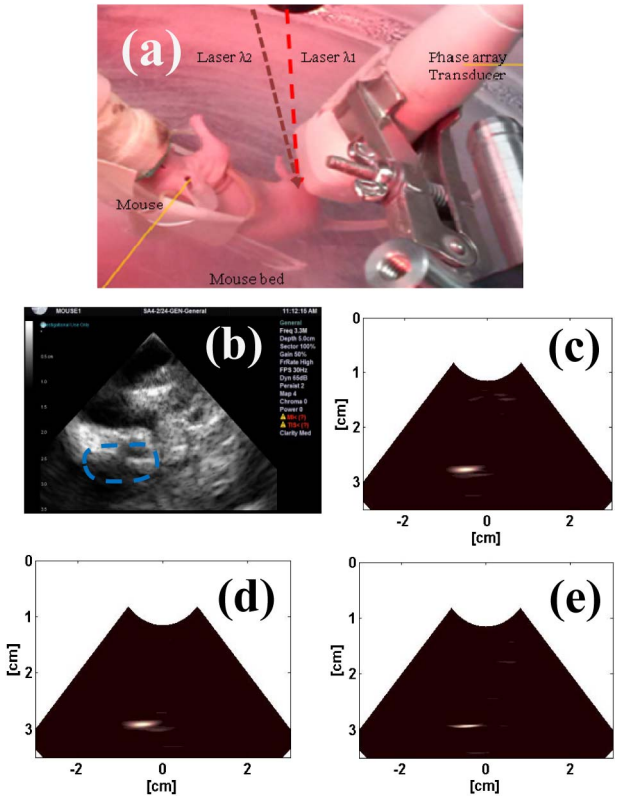

Fig. 3. FD-PA imaging of cancerous tumor in a mouse thigh: (a) the mouse leg and transducer are placed inside the water tank and the laser beams emit from the top. (b) Ultrasonic image of the mouse thigh using a commercial ultrasonic system. (c) FD-PA image obtained with the 805 nm laser only. (d) FD-PA image based on the 805 nm laser modulation waveform with both lasers emitting simultaneously. (e) FD-PA image based on the 680 nm waveform with both lasers emitting simultaneously.

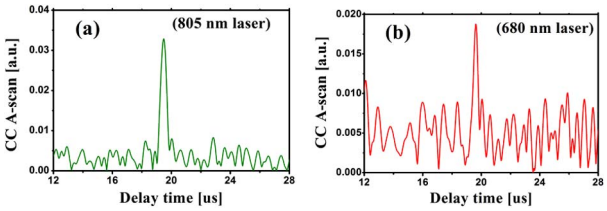

Fig. 4. Scans from one array element corresponding to the maximum FD-PA signal in (a) 805 nm laser and (b) 680 nm laser with both lasers emitting simultaneously.

ultrasonic imaging for comparison. The PA images were reconstructed using a phased-array reconstruction algorithm modified for PA [21]. The ultrasonic image of the mouse thigh and tumor, as well as PA images with 805 nm (emitted alone) are shown in Figs. 3(b) and 3(c), respectively. Figures 3(d) and 3(e) show the PA images using 805 nm and 680 nm wavelengths, respectively, while being emitted simultaneously. Similar to Fig. 2, here the comparison between Figs. 3(c) and 3(d) shows the effect on the generated image of adding another laser with mismatched modulation. The ultrasound image, Fig. 3(b), shows the location of the tumor (highlighted). The photoacoustic images exhibited the tumor vascularization area with much superior contrast. Figure 4 shows the PA cross-correlation signal from one element (out of 64) of the transducer. By normalizing the signal peaks with their corresponding laser fluences, sO_2 can be estimated (similar to the previous experiment) to be 71% in the tumor location. No compensation for light fluence variations was performed here, as the tumor was not located in deep tissue. In general, the proposed method does not generate any advantage or disadvantage in this regard.

In summary, in this work we demonstrated the feasibility of performing simultaneous multi-spectral PA imaging with multiple mismatched excitation chirp waveforms operating simultaneously. Using waveform engineering in the form of two laser modulations with mismatched coded excitations, we could distinguish the PA response at each wavelength separately with minimum or no interference from the other laser. This is a unique feature of FD-PA that can facilitate speed and accuracy of PA functional imaging using multi-spectral methods.

The authors gratefully acknowledge the support of the Canada Research Chairs program and the Natural Sciences and Engineering Research Council of Canada (NSERC) for a Discovery Grant and a 2013–2016 CHRP (NSERC—CIHR) Grant to A.M. We thank Drs. Willa Shi and Fei-Fei Liu of the Ontario Cancer Research, and Princess Margaret Hospital, for their help with culturing the FaDu cells. We also thank the Division of Comparative Medicine (DCM) of Faculty of Medicine of University of Toronto, and particularly Ms. Jennifer Martin for her help with animal preparation, cell injection, anesthesia, and euthanasia.

References

1. S. A. Telenkov, A. Mandelis, B. Lashkari, and M. Forcht, J. Appl. Phys. **105**, 102029, 2009.
2. K. Maslov and L. V. Wang, J. Biomed. Opt. **13**, 024006, 2008.
3. B. Lashkari and A. Mandelis, Opt. Lett. **35**, 1623 (2010).
4. P. Mohajerani, S. Kellnberger, and V. Ntziachristos, J. Photoacoust. **2**, 111 (2014).
5. S. Hu and L. V. Wang, J. Biomed. Opt. **15**, 011101 (2010).
6. B. Cox, J. G. Laufer, S. R. Arridge, and P. C. Beard, J. Biomed. Opt. **17**, 061202 (2012).
7. T. J. Allen, A. Hall, A. P. Dhillon, J. S. Owen, and P. C. Beard, J. Biomed. Opt. **17**, 061209 (2012).
8. X. Wang, X. Xie, G. Ku, L. V. Wang, and G. Stoica, J. Biomed. Opt. **11**, 024015 (2006).
9. G. M. Spirou, A. Mandelis, I. A. Vitkin, and W. M. Whelan, Appl. Opt. **47**, 2564 (2008).
10. V. Ntziachristos and D. Razansky, Chem. Rev. **110**, 2783 (2010).
11. A. Buehler, M. Kacprowicz, A. Taruttis, and V. Ntziachristos, Opt. Lett. **38**, 1404 (2013).
12. M. P. Mienkina, C. S. Friedrich, N. C. Gerhardt, M. F. Beckmann, M. F. Schiffner, M. R. Hofmann, and G. Schmitz, Opt. Express **18**, 9076 (2010).
13. J.-M. Yang, C. Favazza, R. Chen, J. Yao, X. Cai, K. Maslov, Q. Zhou, K. K. Shung, and L. V. Wang, Nat. Med. **18**, 1297 (2012).
14. X. L. Deán-Ben, E. Bay, and D. Razansky, Sci. Rep. **4**, 5878 (2014).
15. T. Misaridis and J. A. Jensen, IEEE Trans. Ultrason. Ferroelectr. Freq. Control **52**, 207 (2005).
16. B. Lashkari, K. Zhang, and A. Mandelis, "High frame rate synthetic aperture ultrasound imaging using mismatched coded excitation waveform engineering: a feasibility study," IEEE Trans. Ultrason. Ferroelect. Freq. Control, submitted.
17. B. Lashkari and A. Mandelis, J. Acoust. Soc. Am. **130**, 1313 (2011).
18. W. G. Zijlstra, A. Buursma, and O. W. van Assendelft, *Visible and Near Infrared Absorption Spectra of Human and Animal Haemoglobin* (VSP, 2000).
19. K. Briley-Sæbø and A. Bjørnerud, Proc. Int. Soc. Magn. Reson. Med. **8**, 2025 (2000).
20. S. Telenkov, R. Alwi, A. Mandelis, and A. Worthington, Opt. Lett. **36**, 4560 (2011).
21. J. A. Jensen, S. I. Nikolov, K. L. Gammelmark, and M. H. Pedersen, Ultrason. J. **44**, e5 (2006).